Potassium Ions Enhance Guanine Radical Generation upon Absorption of Low-Energy Photons by G-quadruplexes and Modify Their Reactivity

Behnaz Behmand,[1§] Evangelos Balanikas, [1] Lara Martinez-Fernandez, [2] Roberto Improta, [3]*

*Akos Banyasz,[4] Gérard Baldacchino[1] and Dimitra Markovitsi[1]**

1. Université Paris-Saclay, CEA, CNRS, LIDYL, F-91191 Gif-sur-Yvette, France

2. Departamento de Quiímica, Facultad de Ciencias, Modúlo13, Universidad Autónoma de Madrid, Campus de Excelencia UAM-CSIC, Cantoblanco, 28049 Madrid, Spain; IADCHEM. Institute for Advanced Research in Chemistry, Universidad Autónoma de Madrid, 28049 Cantoblanco, Madrid, Spain

3. Istituto Biostrutture e Bioimmagini- Consiglio Nazionale delle Ricerche, Via Mezzocannone 16, I-80134 Napoli, Italy

4. Univ Lyon, ENS de Lyon, CNRS UMR 5182, Université Claude Bernard Lyon 1, Laboratoire de Chimie, F-69342 Lyon, France

Corresponding Authors

*lara.martinez@uam.es; dimitra.markovitsi@cea.fr

---

1. Experimental details

Sample preparation and handling

TGGGGT oligonucleotides, purified by reversed phase HPLC and tested by MALDI-TOF, were purchased from Eurogentec Europe. They were dissolved in phosphate buffer (0.15 mol L^{-1} KH_2PO_4, 0.15 mol L^{-1} K_2HPO_4); the purity of both potassium salts (Fluka) used for the buffer was 99.999%. Solutions were prepared using ultrapure water delivered by a MILLIPORE (Milli-Q Integral) system; the pH, measured by a HANNA Instr. Apparatus (pH 210), was adjusted to 7 by addition of a concentrated KOH solution. A 2 mL mother solution was heated to 96°C during 5 min in a dry bath (Eppendorf-ThermoStatplus); subsequently, the solution was cooled to 4°C (cooling time: 2h), where it was incubated overnight.

$(TG4T)_4/K^+$ solutions were kept at -20°C. Prior to time-resolved experiments, they were heated to 40°C and cooled slowly to room temperature. During the experiments the temperature was maintained at 23°C. The absorbance on the excitation side was 0.25 ± 0.02 over 0.1 cm, corresponding to a concentration of about $1.5x10^{-5}$ $molL^{-1}$.

The entire study required the use of six different batches of oligonucleotides. The reproducibility of the results was checked by making control experiments at selected wavelengths. Control experiments were also performed to compare the behavior of **$(TG4T)_4/K^+$** and **$(TG4T)_4/Na^+$**, prepared with the same batch.

Spectroscopic measurements

Steady-state absorption spectra were recorded using a Lambda 850 (Perkin-Elmer) spectrophotometer. The transient absorption setup used as excitation source the fourth harmonic of a Nd:YAG laser (Spectra-Physics, Quanta Ray). The excited area at the surface of the sample and the optical path-length on the excitation side were, respectively, 0.6 × 1.0 cm^2 and 0.1 cm. The analyzing beam, orthogonal to the exciting beam, was provided by a 150 W Xe-arc lamp (OSRAM XBO); its optical path-length through the sample was 1 cm while its thickness was limited to 0.1 cm in order to use the most homogeneous part of the light. It was dispersed in a Jobin-Yvon SPEX 270M monochromator, detected by a Hamamatsu R928 photomultiplier and recorded by a Lecroy Waverunner oscilloscope (6084). For measurements on the sub µs-scale the Xe-arc lamp was intensified via an electric discharge. Transient absorption spectra were recorded using a wavelength-by-wavelength approach. Fast shutters were placed in the path of both laser and lamp beams; thus, the excitation rate was decreased from 10 Hz to 0.2 Hz. The incident pulse energy at the surface of the sample was measured using a NIST traceable pyroelectric sensor (OPHIR Nova2/PE25); potential variations during a measurement were monitored by detecting a fraction of the exciting beam by a photodiode. In addition, the absorbance of the

naphthalene triplet state, whose quantum yield in cyclohexane is 0.75, served as actinometer.[1] At each wavelength, a series of three successive signals, resulting from 20-50 laser shots each, were recorded; if judged to be reproducible they were averaged to reduce the signal-to-noise ratio.

2. Computational details

CASPT2/CASSCF.

The ground state equilibrium geometry of guanine in gas phase (Figure SI-2a) was optimized at the Complete Active Space Self Consistent Field (CASSCF)[2] level of theory using the ANO-S[3-4] basis set and an active space containing 14 electrons in 11 orbitals (Figure SI-3). This active space contains the entire π system and the lone pair of the carbonyl group. Using this optimized geometry as reference, the VIP value was predicted by computing the energy difference of the neutral and cationic species arising from respective single points at the CASPT2 level of theory (multistate second order perturbation theory on state average complete active space self-consistent field wavefunctions).[5-6] An imaginary level shift[7] of 0.3 a.u. was used and two different IPEA values (0.25 and 0.0 a.u.) were considered[8] giving VIP values of 8.27 and 8.10 eV, respectively. All the calculations were done with OpenMolcas.[9]

DFT and TD-DFT.

Guanine. For comparison with the CASPT2 energies, the ground state of guanine was optimized at the M052X/6-31G(d)[10-11] level of theory in gas phase and its VIP simulated at the same level of theory. This functional has been successfully applied in previous studies to optimize guanine radicals and to simulate their absorption spectra.[12-15]

$(TG4T)_4/K^+$. Ground state and radical species were optimized through a QM/MM approach, in which three of the four guanine tetrads and two K^+ are treated at the QM level, whereas the fourth tetrad (and the corresponding K^+), the backbone and external K^+ ions were considered at the MM level (Figure SI-2b). The QM part was described at the DFT(M052X)/6-31G(d) level of theory. For the MM region we selected Amber parm96.dat Force Field.[16] In this case, the whole system was embedded in solvent using the Polarizable Continuum Model.[17-18] Absorption spectra of the radicals were simulated calculating the vertical absorption energies using TD-DFT and convoluting each transition with a Gaussian function of half width half maximum of 0.3 eV.

For the VIP, single point calculations on top of the ground state of **$(TG4T)_4/K^+$** and **$(TG4T)_4/Na^+$** were performed.

All these calculations were done with Gaussian 09.[19]

3. Additional Figures

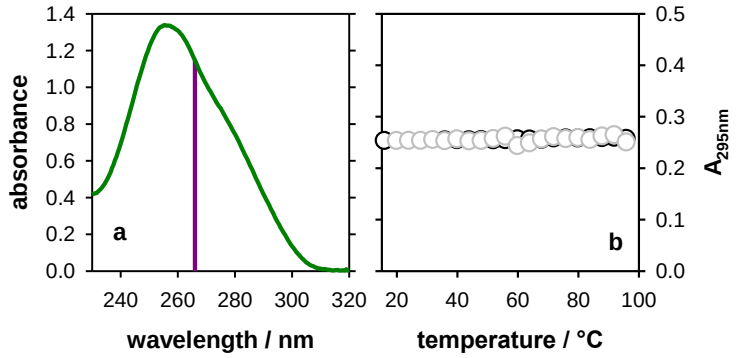

Figure SI-1. (a) Absorption spectrum of **(TG4T)$_4$/K$^+$** at 23°C; the violet vertical line indicates the laser excitation wavelength. (**b**) Absorbance of **(TG4T)$_4$/K$^+$** at 295 nm as a function of temperature; black and grey circles correspond to independent measurements performed with different oligomer batches.

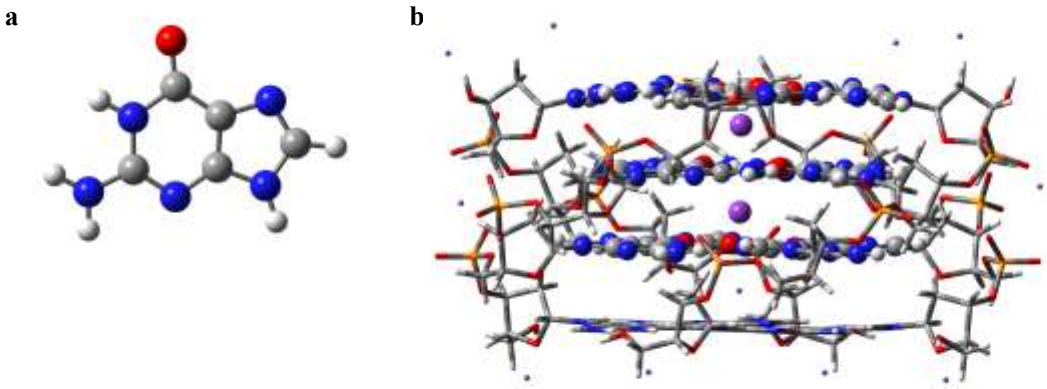

Figure SI-2. Computational models used for (**a**) guanine nucleobase and (**b**) **(TG4T)$_4$/K$^+$**; QM atoms are shown in ball and stick, while MM ones are depicted as tubes.

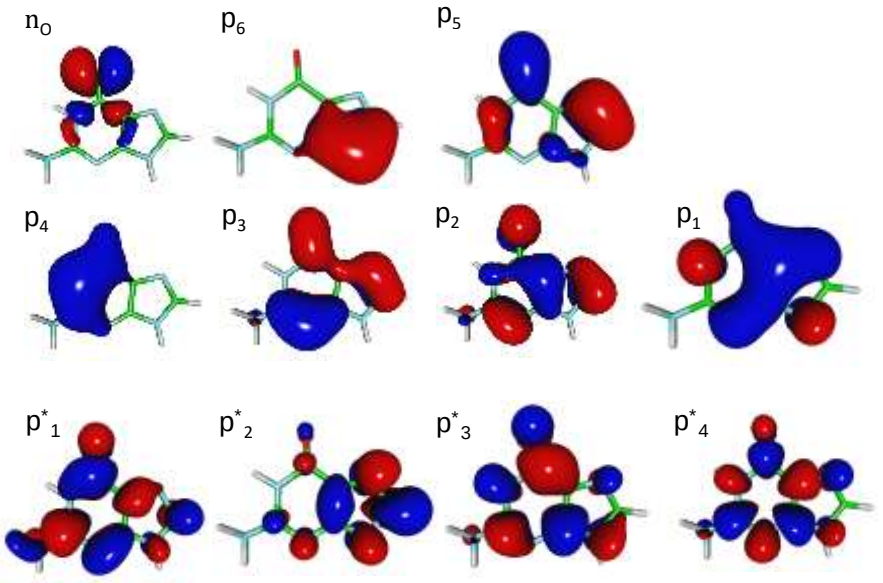

Figure SI-3. Molecular orbitals involved in the (14,11) active space used for CASSCF calculations.

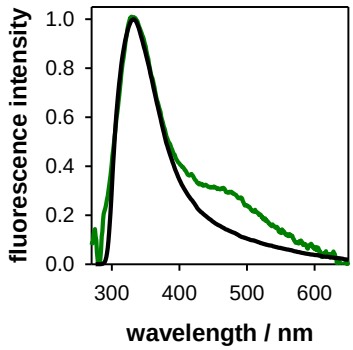

Figure SI-4. Steady-state fluorescence spectrum obtained for the dinucleotides dGpT, purified by reversed phase HPLC (green) and an equimolar mixture of mononucleotides dGMP and TMP (black). Excitation wavelength: 255 nm.

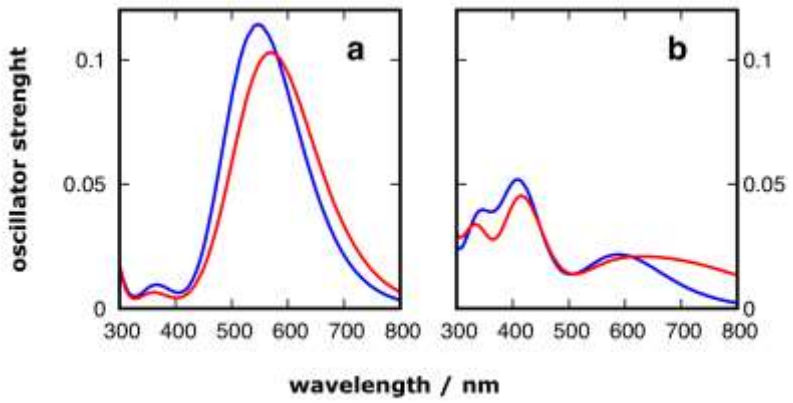

Figure SI-5. Comparison of the absorption spectra computed for the deprotonated radicals of **(TG4T)$_4$/K$^+$** (blue) and **(TG4T)$_4$/Na$^+$** (red): (**a**) (**G**-H2)$^\bullet$ and (**b**) (**G**-H1)$^\bullet$ at the TD-M052X/6-31G(d) level of theory.

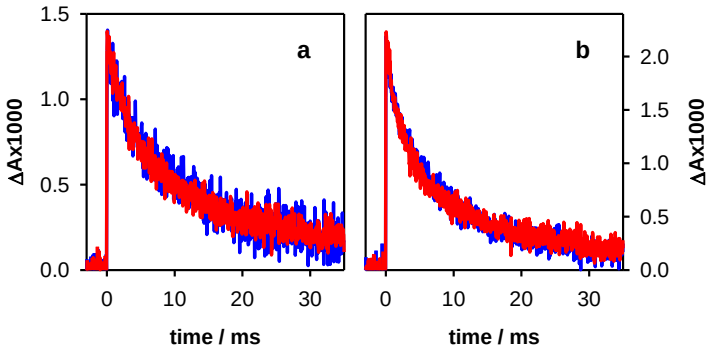

Figure SI-5. Transient absorption decays recorded at 605 nm for **(TG4T)$_4$/K$^+$** in concentrated (red: 0.15 mol L^{-1} KH_2PO_4, 0.15 mol L^{-1} K_2HPO_4) and diluted (blue: 0.015 mol L^{-1} KH_2PO_4, 0.015 mol L^{-1} K_2HPO_4) obtained using 3mJ (**a**) and 6 mJ (**b**) laser pulses at 266 nm. The signals are not normalized.

References

1. Amand, B.; Bensasson, R. Determination of triplet quantum yields by laser flash absorption spectroscopy. *Chem. Phys. Lett.* **1975,** *34*, 44-48.
2. Roos, B. O. Ab initio Methods in Quantum Chemistry Lawley, K. P., Ed. Wiley, Chichester: 1987; Vol. II.
3. Pierloot, K.; Dumez, B.; Widmark, P. O.; Roos, B. O. Density matrix averaged atomic natural orbital (ANO) basis sets for correlated molecular wave function. *Theor. Chem. Act.* **1995,** *90*, 87-114
4. Lorentzon, J.; Malmqvist, P. A.; Fulscher, M.; Roos, B. O. A CASPT2 Study of the Valence and Lowest Rydberg Electronic States of Benzene and Phenol. *Theor. Chem. Act.* **1995,** *91*, 91-108.
5. Andersson, K.; Malmqvist, P. A.; Roos, B. O. 2nd-order Perturbation Theory with a Complete Active Space Self-Consistent Field Reference Function. *J. Chem. Phys.* **1992,** *96*, 1218-1226.
6. Finley, J.; Malmqvist, P. A.; Roos, B. O.; Serrano-Andres, L. The multi-state CASPT2 method. *Chem. Phys. Lett.* **1998,** *288*, 299-306.
7. Forsberg, N.; Malmqvist, P. A. Multiconfiguration perturbation theory with imaginary level shift. *Chem. Phys. Lett.* **1997,** *274*, 196-204.
8. Ghigo, G.; Roos, B. O.; Malmqvist, P. A. A modified definition of the zeroth-order Hamiltonian in multiconfigurational perturbation theory (CASPT2). *Chem. Phys. Lett.* **2004,** *396*, 142-149.

9. Galvan, I. F.; Vacher, M.; Alavi, A.; Angeli, C.; Aquilante, F.; Autschbach, J.; Bao, J. J.; Bokarev, S. I.; Bogdanov, N. A.; Carlson, R. K.; Chibotaru, L. F.; Creutzberg, J.; Dattani, N.; Delcey, M. G.; Dong, S. J. S.; Dreuw, A.; Freitag, L.; Frutos, L. M.; Gagliardi, L.; Gendron, F.; Giussani, A.; Gonzalez, L.; Grell, G.; Guo, M. Y.; Hoyer, C. E.; Johansson, M.; Keller, S.; Knecht, S.; Kovacevic, G.; Kallman, E.; Li Manni, G.; Lundberg, M.; Ma, Y. J.; Mai, S.; Malhado, J. P.; Malmqvist, P. A.; Marquetand, P.; Mewes, S. A.; Norell, J.; Olivucci, M.; Oppel, M.; Phung, Q. M.; Pierloot, K.; Plasser, F.; Reiher, M.; Sand, A. M.; Schapiro, I.; Sharma, P.; Stein, C. J.; Sorensen, L. K.; Truhlar, D. G.; Ugandi, M.; Ungur, L.; Valentini, A.; Vancoillie, S.; Veryazov, V.; Weser, O.; Wesolowski, T. A.; Widmark, P. O.; Wouters, S.; Zech, A.; Zobel, J. P.; Lindh, R. OpenMolcas: From Source Code to Insight. *J. Chem. Theory Comput.* **2019,** *15*, 5925-5964.
10. Zhao, Y.; Schultz, N. E.; Truhlar, D. G. Design of density functionals by combining the method of constraint satisfaction with parametrization for thermochemistry, thermochemical kinetics, and noncovalent interactions. *J. Chem. Theory Comput.* **2006,** *2*, 364-382.
11. Zhao, Y.; Truhlar, D. G. Density functionals with broad applicability in chemistry. *Acc. Chem. Res.* **2008,** *41*, 157-167.
12. Banyasz, A.; Balanikas, E.; Martinez-Fernandez, L.; Baldacchino, G.; Douki, T.; Improta, R.; Markovitsi, D.; 2019. Radicals generated in tetramolecular guanine quadruplexes by photo-ionization: spectral and dynamical features. *J. Phys. Chem. B* **2019,** *123*, 4950-4957.
13. Martinez-Fernandez, L.; Banyasz, A.; Markovitsi, D.; Improta, I. Topology controls the electronic absorption delocalization of electron hole in guanine quadruplexes. *Chem. Europ. J.* **2018,** *24*, 15185-15189.
14. Banyasz, A.; Martinez-Fernandez, L.; Improta, R.; Ketola, T. M.; Balty, C.; Markovitsi, D. Radicals generated in alternating guanine-cytosine duplexes by direct absorption of low-energy UV radiation. *Phys. Chem. Chem. Phys.* **2018,** *20*, 21381-21389.
15. Banyasz, A.; Martinez-Fernandez, L.; Balty, C.; Perron, M.; Douki, T.; Improta, R.; Markovitsi, D. Absorption of Low-Energy UV Radiation by Human Telomere G-Quadruplexes Generates Long-Lived Guanine Radical Cations. *J. Am. Chem. Soc.* **2017,** *139*, 10561-10568.
16. Cornell, W. D.; Cieplak, P.; Bayly, C. I.; Gould, I. R.; Merz, K. M.; Ferguson, D. M.; Spellmeyer, D. C.; Fox, T.; Caldwell, J. W.; Kollman, P. A. A 2nd Generation Force-Field for the Simulation of Proteins, Nucleic Acids and Organic Molecules. *J. Am. Chem. Soc.* **1995,** *117*, 5179-5197.
17. Miertus, S.; Scrocco, E.; Tomasi, J. Electrostatic interaction of a solute with a continuum - A direct utilization of abinitio molecular potentials for the prevision of solvent effects *Chem. Phys.* **1981,** *55*, 117-129.
18. Tomasi, J.; Mennucci, B.; Cammi, R. Quantum mechanical continuum solvation models. *Chem. Rev.* **2005,** *105*, 2999-3093.
19. Frisch, M. J.; Trucks, G. W.; Schlegel, H. B.; Scuseria, G. E.; Robb, M. A.; Cheeseman, J. R.; Scalmani, G.; Barone, V.; Mennucci, B.; Petersson, G. A.; Nakatsuji, H.; Caricato, M.; Li, X.; Hratchian, H. P.; Izmaylov, A. F.; Bloino, J.; Zheng, G.; Sonnenberg, J. L.; Hada, M.; Ehara, M.; Toyota, K.; Fukuda, R.; Hasegawa, J.; Ishida, M.; Nakajima, T.; Honda, Y.; Kitao, O.; Nakai, H.; Vreven, T.; Montgomery, J. A.; Peralta, J. J. E.; Ogliaro, F.; Bearpark, M.; Heyd, J. J.; Brothers, E.; Kudin, K. N.; Staroverov, V. N.; Kobayashi, R.; Normand, J.; Raghavachari, K.; Rendell, A.; Burant, J. C.; Iyengar, S. S.; Tomasi, J.; Cossi, M.; Rega, N.; Millam, J. M.; Klene, M.; Knox, J. E.; Cross, J. B.; Bakken, V.; Adamo, C.; Jaramillo, J.; Gomperts, R.; Stratmann, R. E.; Yazyev, O.; Austin, A. J.; Cammi, R. C.; Pomelli, C.; Ochterski, J. W.; Martin, R. L.; Morokuma, K.; Zakrzewski, V. G.; Voth, G. A.; Salvador, P.; Dannenberg, J. J.; Dapprich, S.; Daniels, A. D.; Farkas, O.; Foresman, J. B.; Ortiz, J. V.; Cioslowski, J.; Fox, D. J. *Gaussian 09, revision A.02*. Gaussian Inc.: Wallingford CT, 2009.